Supplementary Material

Site-specific isotope labeling of long RNA for structural and mechanistic studies

Ikumi Kawahara[1,2], Kaichiro Haruta[1,#,*], Yuta Ashihara[1], Daichi Yamanaka[1], Mituhiro Kuriyama[1], Naoko Toki[1], Yoshinori Kondo[1], Kenta Teruya[3], Junya Ishikawa[4], Hiroyuki Furuta[4], Yoshiya Ikawa[4], Chojiro Kojima[2,5], Yoshiyuki Tanaka[1,*]

[1]Graduate School of Pharmaceutical Sciences, Tohoku University, Sendai 980-8578, Japan
[2]Graduate School of Biological Sciences, NAIST, Ikoma 630-0101, Japan
[3]Graduate School of Medical Science, Kyoto Prefectural University of Medicine, Kyoto 603-8334, Japan
[4]Department of Chemistry and Biochemistry, Graduate School of Engineering, Kyushu University, Fukuoka 819-0395, Japan
[5]Institute for Protein Research, Osaka University, Suita 565-0871, Japan
[#]Present address: Research Center, Mitsui Chemicals, Inc., Japan

Contents:

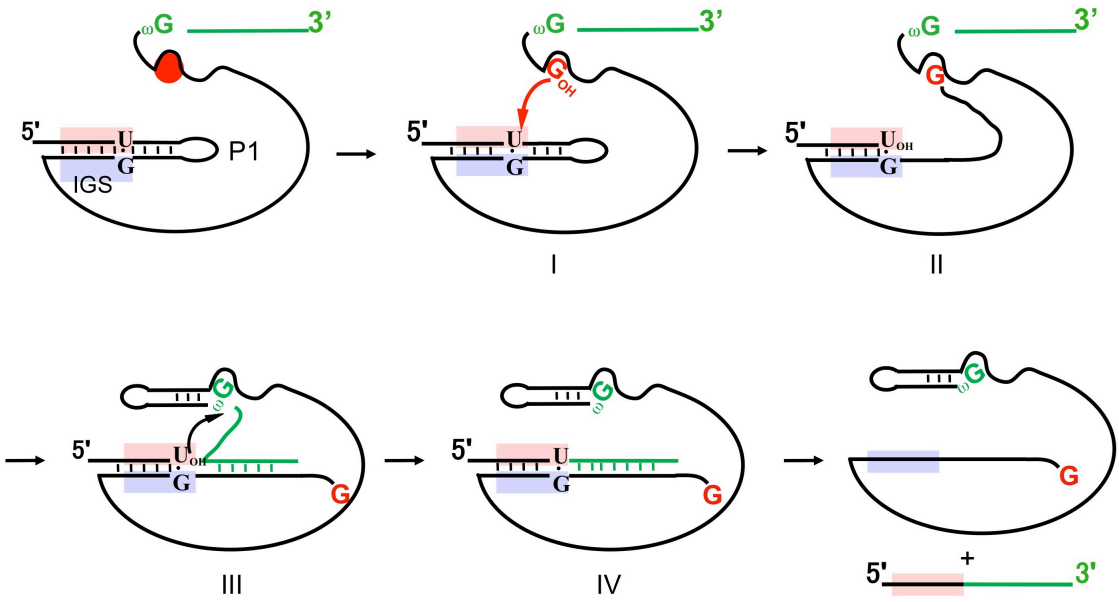

Figure S1. General self-splicing reaction pathway of group I introns. The internal guide sequence (IGS) and anti-IGS are highlighted with blue and pink backgrounds, respectively. The 3' exon with ωG and the remainder of the sequence are colored in green and black, respectively. External guanosine and its binding site within the intron are colored in red. When using the cis-acting group I intron for a guanosine transfer reaction, the external guanosine will be introduced at the 5'-end of the intron itself (state II) (39, 44). To obtain 5'-end labeled RNA fragments from this group I intron, its 5' sequence needs to be cleaved at the appropriate site, which requires extra steps. However, when using the trans-acting group I intron, this cleavage step can be skipped, and 5'-end labeled RNA can be derived immediately after the guanosine transfer reaction as shown in Figure 1b.

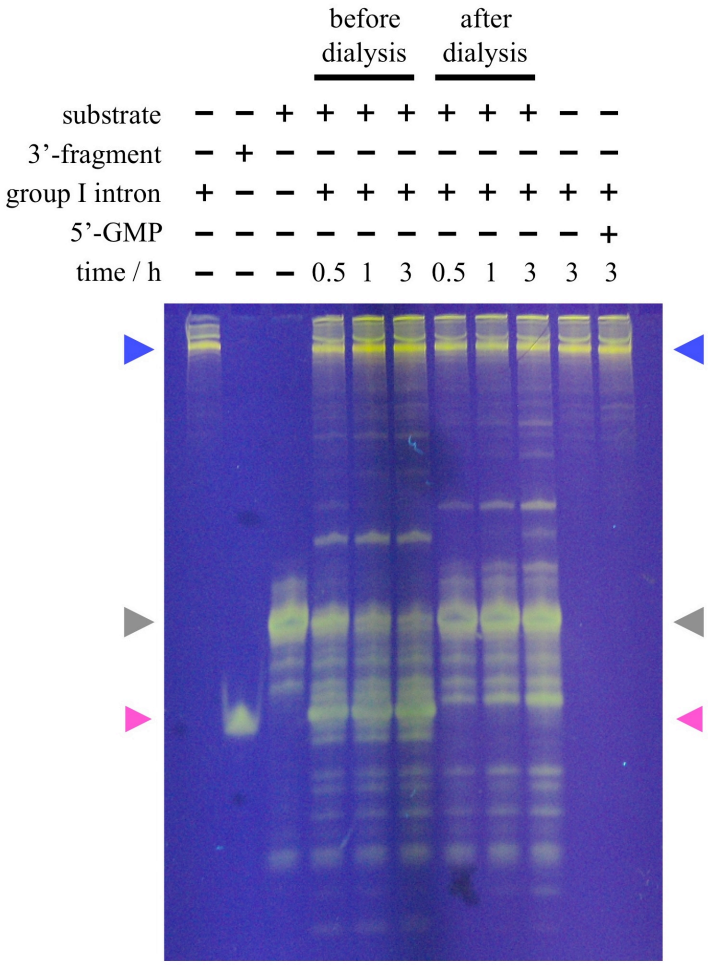

Figure S2. Sampling of group I intron with dialysis. The group I intron solution contained excess 5'-NTP after in vitro transcription, which may result in an undesired background guanosine transfer reaction with non-labeled 5'-GTP. Therefore, we examined whether dialysis can remove co-existing 5'-GTP from the group I intron solution. Lanes 4-6: reactions before dialysis. Lanes 7-9: reactions after dialysis. Blue arrowheads indicate *Tetrahymena* group I intron, gray arrowheads indicate the 3' fragment precursor and pink arrowheads indicate 3' fragment after the guanosine transfer. As shown in lanes 4-6, background guanosine transfer reaction with non-labeled 5'-GTP took place, whereas after dialysis this undesired side reaction was suppressed. Reaction mixtures contained 50 μM 3' fragment precursor, 30 mM Tris-HCl pH 7.2, 10 mM NH_4Cl, 3 mM $MgCl_2$ and 1.4 μM *Tetrahymena* group I intron with or without dialysis (lanes 4-9). The control reaction (lane 10) contained 1.4 μM dialyzed group I intron in the same buffer without 3' fragment precursor; the second control reaction (lane 11) contained 1.4 μM dialyzed group I intron and 2 mM 5'-GMP in the same buffer without substrate. All reactions were carried out at 53 °C.

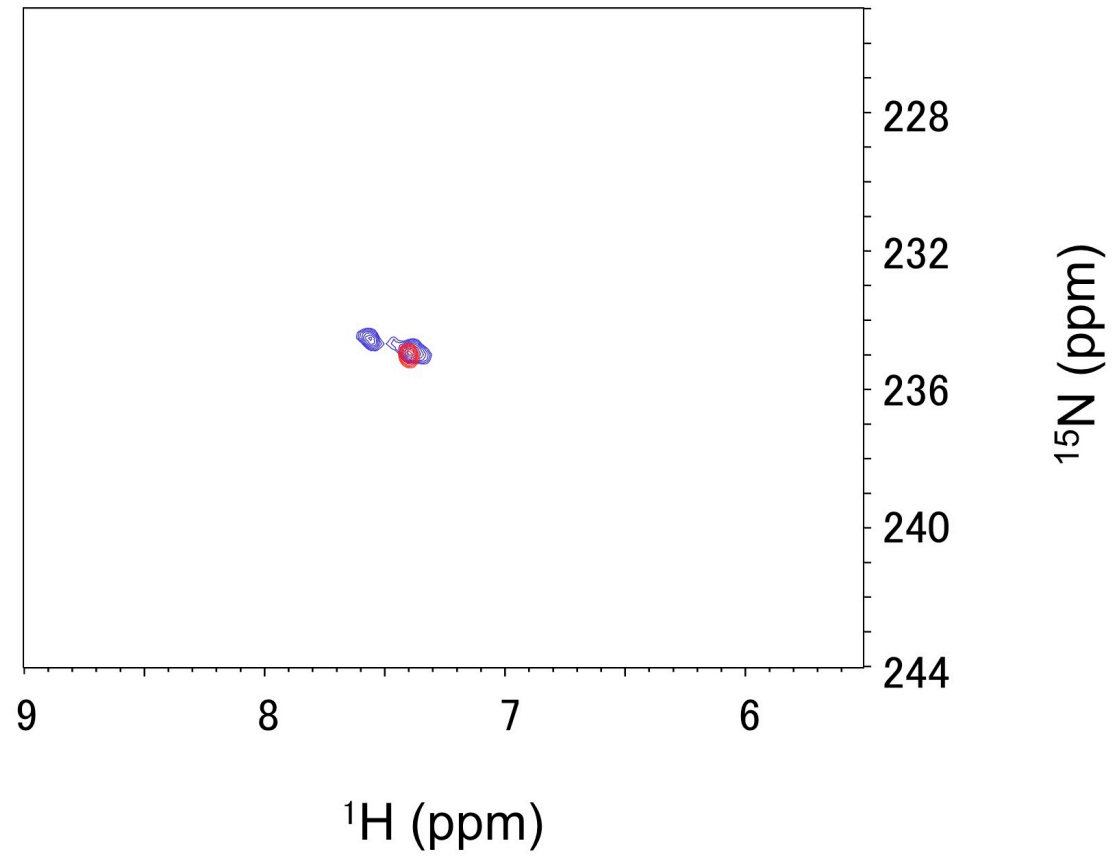

Figure S3. Overlay of H8-N7 cross peak region of ^{1}H-^{15}N HSQC spectra of substrate-free and substrate-bound hammerhead ribozyme. Substrate-free and substrate-bound states are colored in red and blue, respectively. In the substrate-bound state (blue), twin peaks were observed. One of these two peaks overlapped with the original peak of the substrate-free form (red). As one of possibility, the overlapped peak would correspond with the substrate-free form, and the other peak would arise from the substrate-bound form. As another possibility, the ribozyme-substrate complex may have a structural polymorphism. In the substrate (inhibitor) strand, the C17 residue at the cleavage site was substituted with 2'-O-methylcytidine to prevent the cleavage reaction with the hammerhead ribozyme (Figures 2a and 3a).

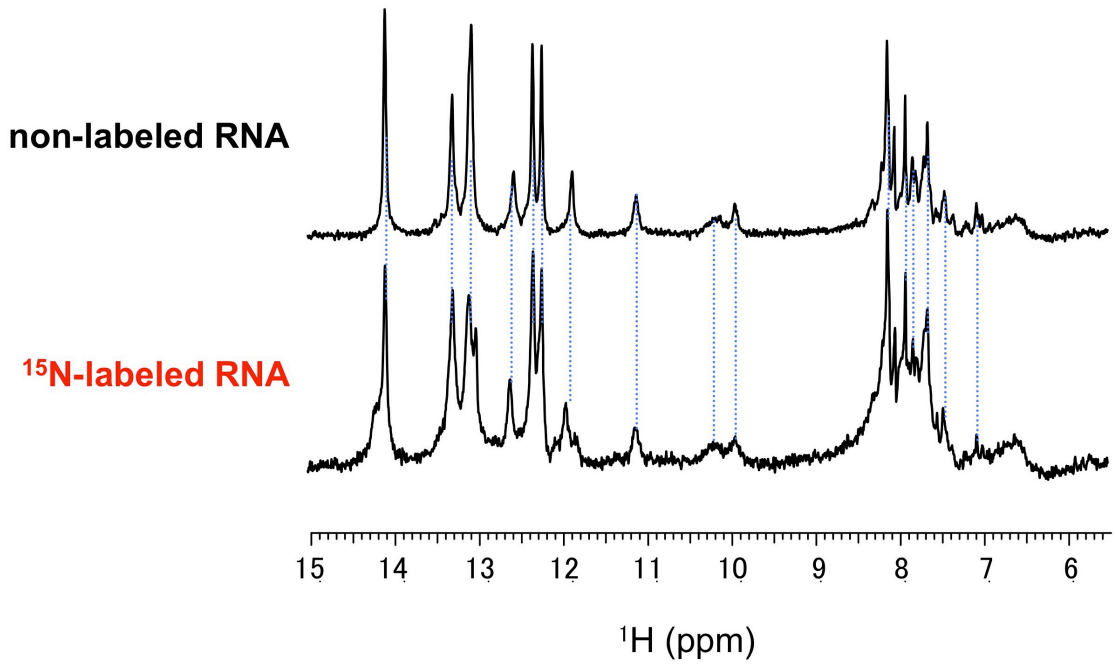

Figure S4. ^{1}H 1D NMR spectra of labeled/non-labeled hammerhead ribozymes. The authentic non-labeled sample (top) and the single-residue labeled sample (bottom).

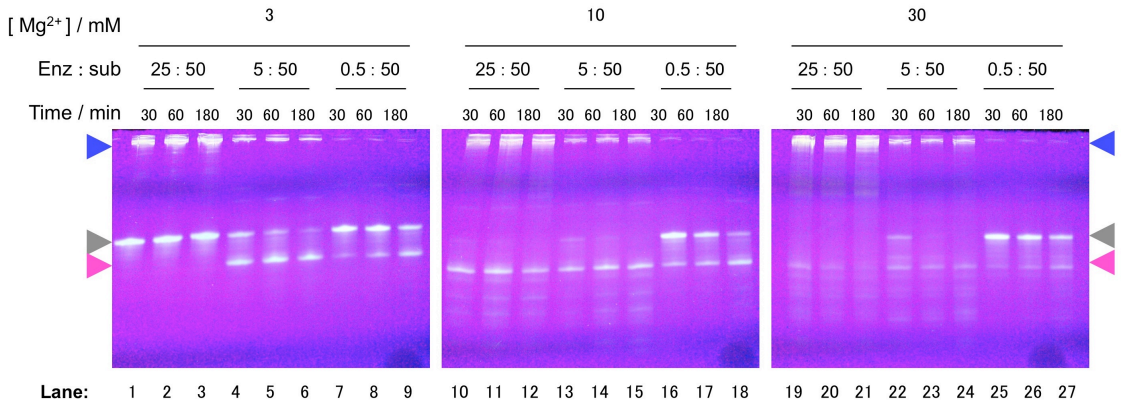

Figure S5. Effects of the concentration of Mg^{2+} and group I intron. The reaction mixture contained 50 μM 3' fragment precursor, 50 mM Tris-HCl pH 7.2, 10 mM NH_4Cl, 2 mM 5'-GMP and various concentrations of $MgCl_2$ (3-30 mM) and *Tetrahymena* group I intron (0.5-25 μM) in a 12 μL final volume. All reactions were carried out at 58 °C. Left panel (lanes 1-9): 3 mM $MgCl_2$. Middle panel (lanes 10-18): 10 mM $MgCl_2$. Right panel (lanes 19-27): 30 mM $MgCl_2$. Blue arrowheads indicate the *Tetrahymena* group I intron, gray arrowheads indicate the 3' fragment precursor and pink arrowheads indicate the 3' fragment after the guanosine transfer. The most efficient reaction was obtained with 3 mM $MgCl_2$ and a 5:50 *Tetrahymena* group I intron/3' fragment precursor ratio (lanes 4-6). At higher concentrations of Mg^{2+} sample degradation was accelerated irrespective of enzyme concentrations (compare lanes 1-9 with lanes 10-15 and 19-24). Moreover, our results demonstrated that when using 3 mM $MgCl_2$, a higher concentration of group I intron (25 μM which corresponds to 10 mM equivalent of backbone phosphate groups) inhibited the reaction (compare lanes 1-3 with lanes 4-6). The assumption that most of the Mg^{2+} ions would be used as counter-ions for the long RNA strand of group I intron and thus less Mg^{2+} ions can be used for the catalysis, may explain these results.

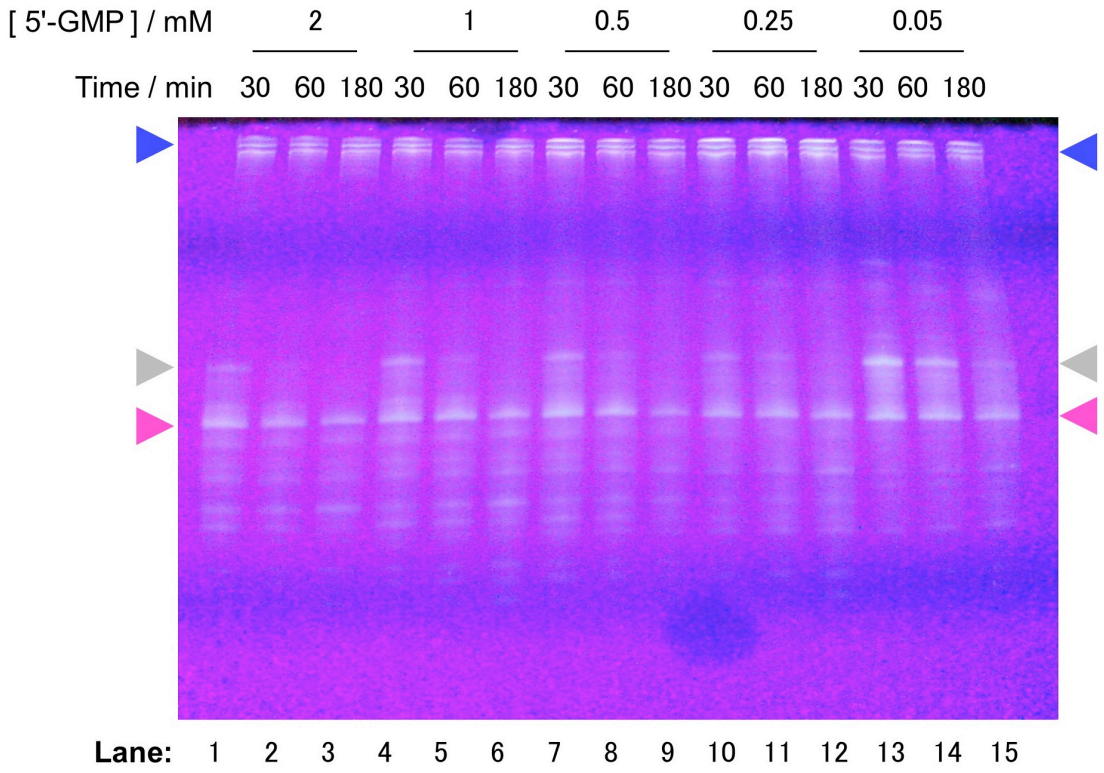

Figure S6. Effects of 5'-GMP concentration. Reaction mixture contained 50 μM 3' fragment precursor, 5 μM *Tetrahymena* group I intron, 30 mM Tris-HCl pH 7.2, 10 mM NH_4Cl, 3 mM $MgCl_2$ and various concentrations of 5'-GMP in a 12 μL final volume. All reactions were carried out at 58 °C. Blue arrowheads indicate *Tetrahymena* group I intron, gray arrowheads indicate the 3' fragment precursor and pink arrowheads indicate 3' fragment after the guanosine transfer. We found that optimal results were obtained with the concentration range of 0.25-2.0 mM 5'-GMP. However, we observed a time-dependent RNA degradation and hence decided to use 2 mM 5'-GMP for NMR sample preparation.

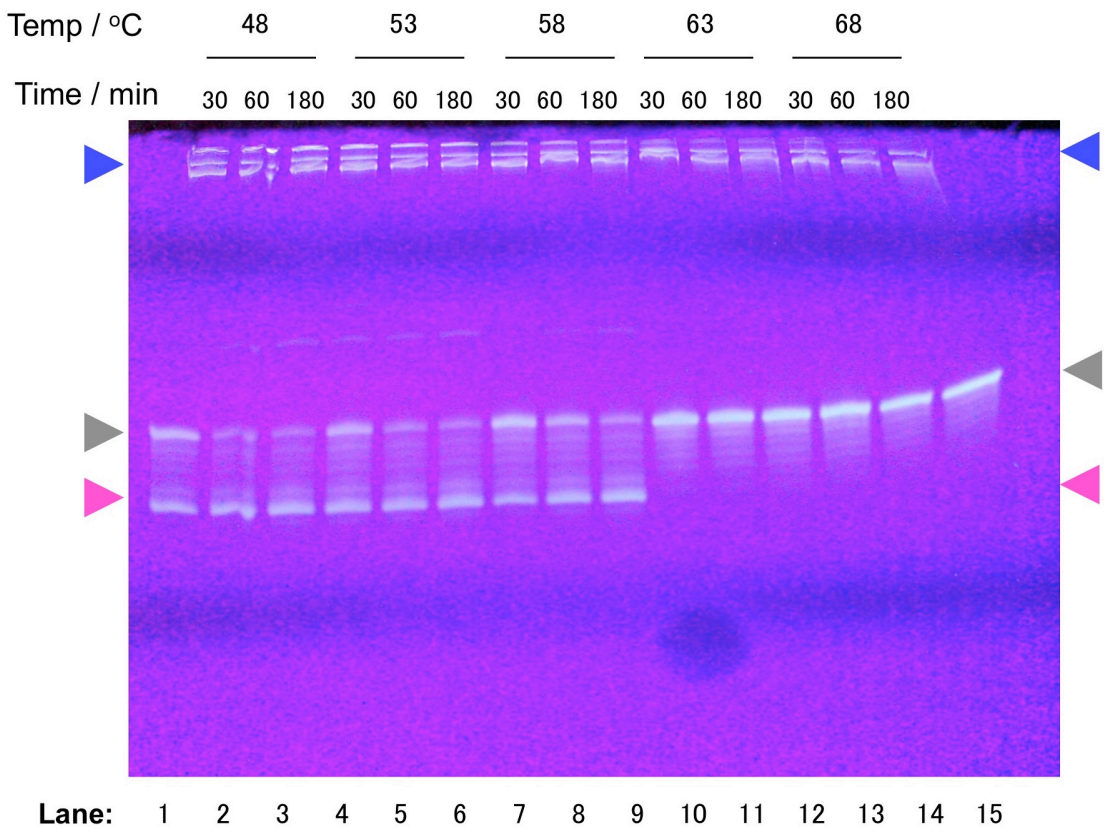

Figure S7. Effects of reaction temperature. Reaction mixture contained 50 μM 3' fragment precursor, 5 μM *Tetrahymena* group I intron, 30 mM Tris-HCl pH 7.2, 10 mM NH_4Cl, 0.5 mM 5'-GMP and 3 mM $MgCl_2$ in a 12 μL final volume. Blue arrowheads indicate *Tetrahymena* group I intron, gray arrowheads indicate the 3' fragment precursor and pink arrowheads indicate 3' fragment after the guanosine transfer. The results suggest that the optimal temperature range for this reaction is 48–58 °C (lanes 1-9), whereas the reaction was completely inhibited in higher temperatures (lanes 10-15). In order to gain high turn over number of the reaction, we chose relatively high temperature for its optimization.

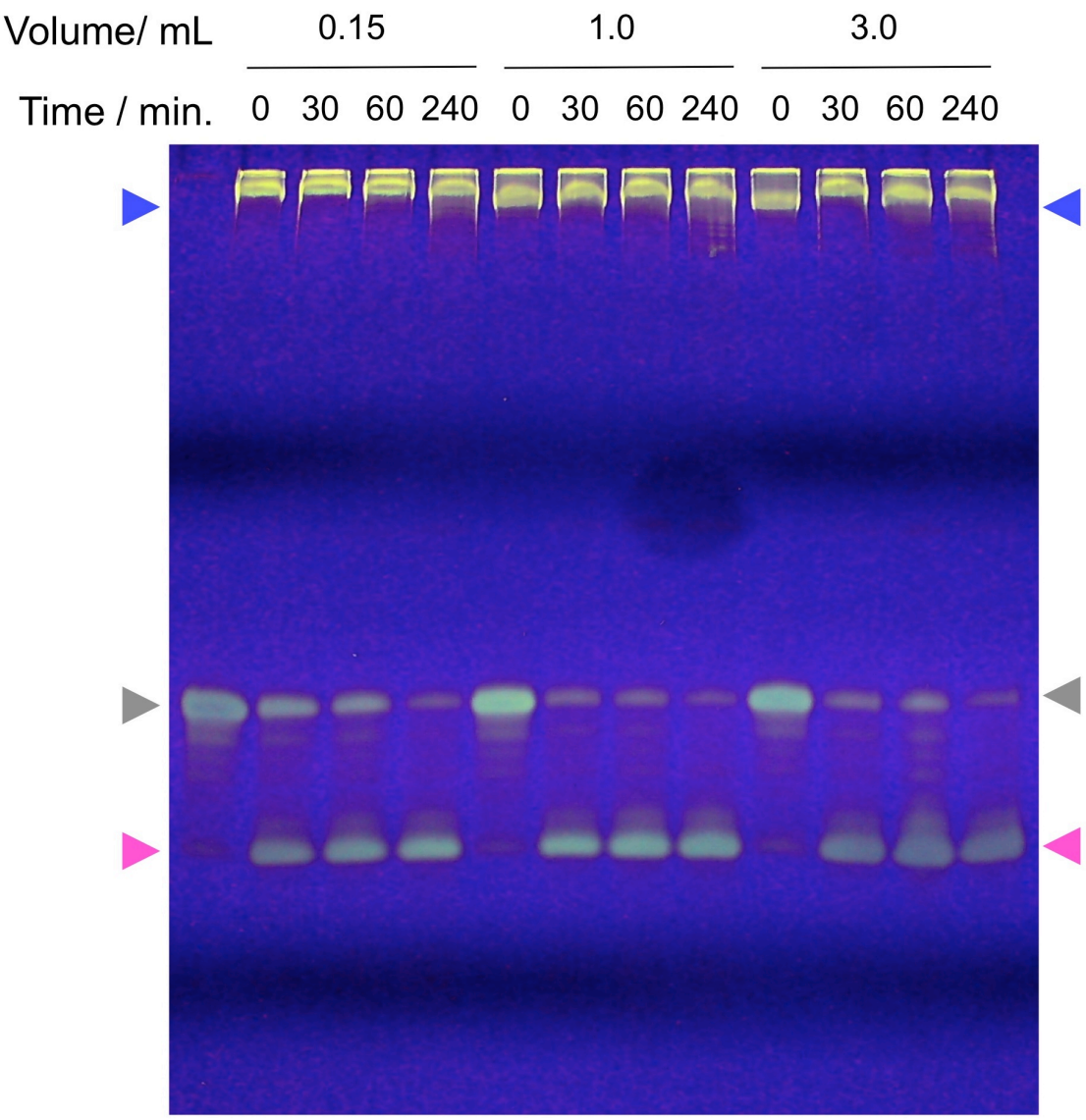

Figure S8. Scale-up of the guanosine transfer reaction. Blue arrowheads indicate *Tetrahymena* group I intron, gray arrowheads indicate the 3' fragment precursor and pink arrowheads indicate the 3' fragment after the guanosine transfer. Each reaction mixture contained 50 μM 3' fragment precursor, 5 μM *Tetrahymena* group I intron, 30 mM Tris-HCl pH 7.2, 10 mM NH_4Cl, 2 mM 5'-GMP and 3 mM $MgCl_2$. All reactions were carried out at 58 °C and followed the general procedure described in Materials and Methods. In this study, reaction volume was scaled up to 3.0 mL without any activity loss of group I intron.

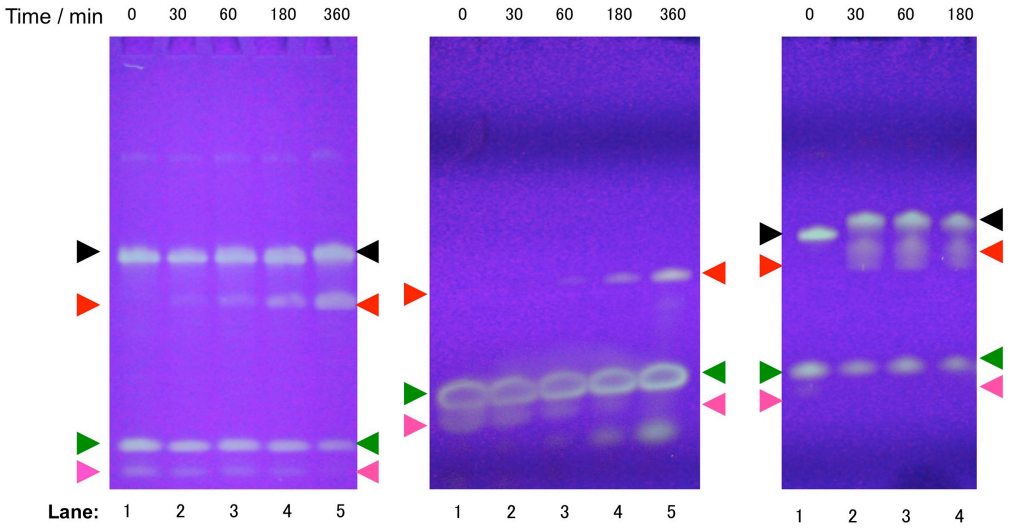

Figure S9. Ligation reactions with various ligases. Left panel: reactions with T4 DNA ligase. Middle panel: reactions with T4 RNA ligase I. Right panel: reactions with T4 RNA ligase II. Red arrowheads show ligated product, black arrowheads show the DNA bridge for ligation, green and pink arrowheads show 5' fragment and 3' fragment substrates of the reaction, respectively. To this end we used the following RNA oligomers: 5' fragment: 5'-CCAGCUGAUGA-3', 3' fragment: 5'-pGUCCCAAAUAG-3' and DNA bridge: 5'-d TCGTCCTATTTGGGACTCATCAGCTGGTAGT-3'. To prepare 5'phosphorylated 3' fragments, we chemically phosphorylated the 5' terminal hydroxy group of the 3' fragment with a phosphorylating reagent (Glen Research, VA, USA). The results show that all the enzymes efficiently catalyzed the ligation reaction of the RNA fragments. In addition to the guanosine transfer reaction, group I intron occasionally promotes a simple RNA hydrolysis reaction, which generates RNA fragments without guanosine at the 5' end. The mis-processed RNA fragments cannot be ligated by a template-dependent ligase (T4 DNA ligase and T4 RNA ligase II), whereas they can be ligated by a template-independent ligase (T4 RNA ligase I). To avoid the incorporation of mis-processed RNA fragments, a template-dependent ligation reaction would be convenient. Thus, in this study we employed T4 DNA ligase. The ligation reaction mixture for T4 RNA ligase I (New England Biolab, MA, USA) contained 10 μM of each RNA oligomer (1 : 1), 50 mM Tris-HCl pH 7.6, 10 mM DTT, 10 mM $MgCl_2$, 1 mM ATP and 20 units T4 RNA ligase I in a reaction volume of 20 μL. The reaction mixture for T4 RNA ligase II (New England Biolabs, MA, USA) contained 10 μM each RNA oligomer (1:1), 15 μM DNA bridge, 50 mM Tris-HCl pH 7.6, 1 mM DTT, 2 mM $MgCl_2$, 400 μM ATP and 10 units T4 RNA ligase II in a reaction volume of 20 μL. The reactions were monitored at the indicated time points by PAGE, containing 8 M urea, and stained with SYBR Gold. The ligation for NMR sample was carried out with T4 DNA ligase as described in experimental section of main text.

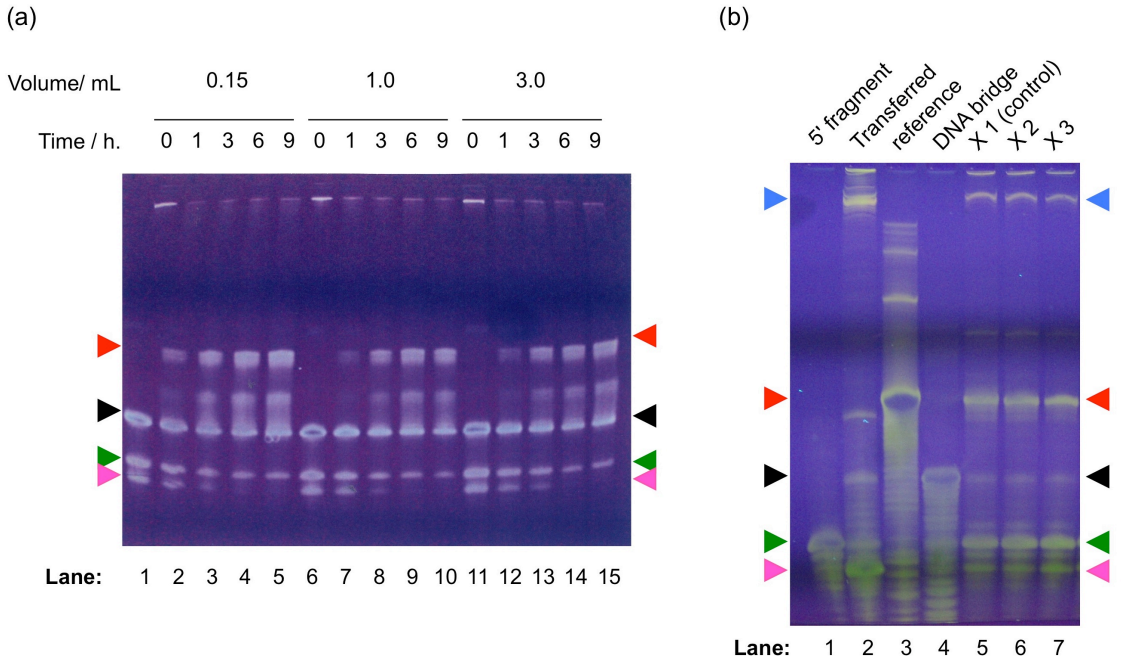

Figure S10. Optimization of ligation conditions. (a) Scale-up of the ligation. Each reaction mixture contained 100 μM 5' fragment, 50 μM 3' fragment, 75 μM DNA bridge, 40 mM Tris-HCl pH 7.6, 10 mM DTT, 10 mM $MgCl_2$, 0.5 mM 5'-ATP and 0.5 units/μL T4 DNA ligase. All reactions were carried out at 37 °C. In this study, reaction volume was scaled up to 3.0 mL without any loss of ligation efficiency. (b) Effects of the concentration of the substrates. The control (lane 5) reaction mixture contained 100 μM 5' fragment, 75 μM DNA bridge, 40 mM Tris-HCl pH 7.6, 10 mM DTT, 10 mM $MgCl_2$, 0.5 mM 5'-ATP, 0.3 units/μL T4 DNA ligase and non-purified guanosine transferred reaction mixture (the estimated concentration of the 3‘ fragment was 50 μM) in a 20 μL final volume. In lanes 6 and 7, concentrations of all the substrate (5'- and 3'-fragmnents and DNA bridge) were twice and 3-times as high as those of the control experiment (lane 5). All reactions were carried out at 37 °C for 8 hours. Arrowheads: (blue) group I intron; (pink) 3' fragment with guanosine; (green) 5' fragment; (black) DNA bridge; (red) ligated RNA (final product) and its reference.

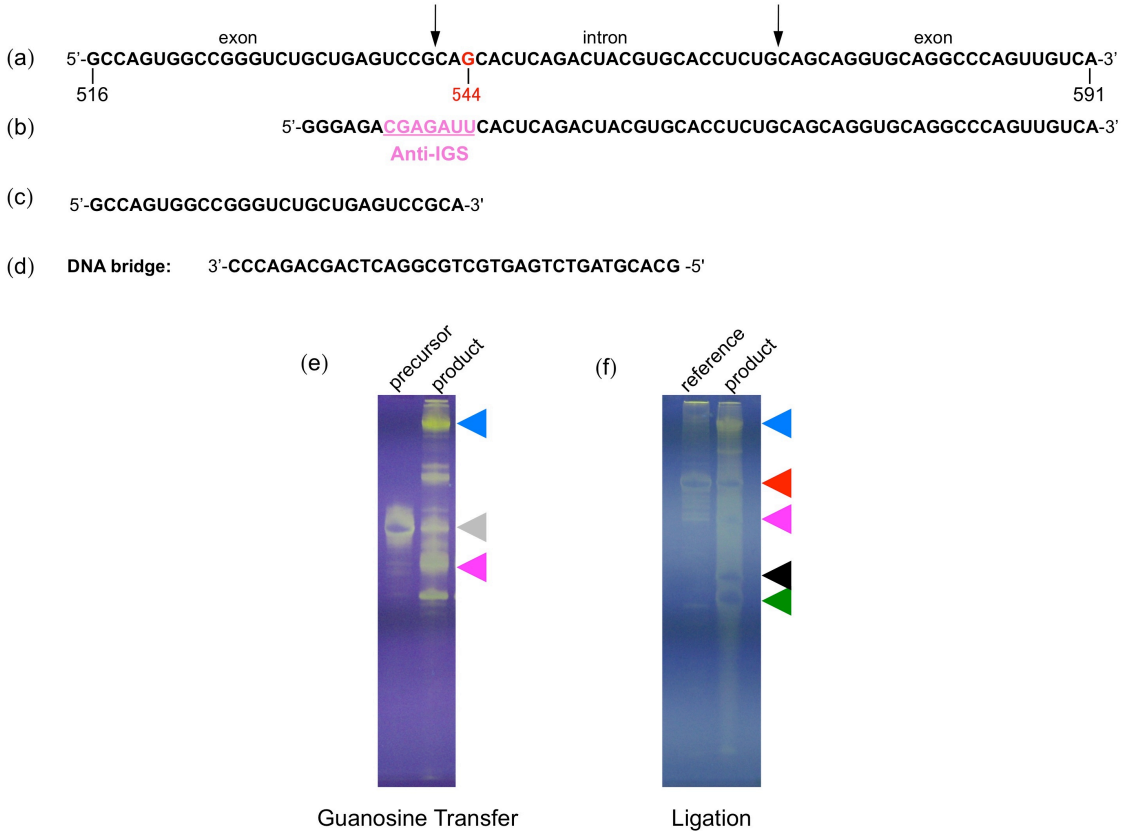

Figure S11. Sample preparation of the single residue-labeled 76-nucleotide RNA molecule (hXBP1 mRNA (516-591)). (a) The sequence of the hXBP1 mRNA (516-591). Nitrogen-15-labeled guanosine residue (G544) is highlighted in red. Black arrows indicate intron-exon junctions. (b) The sequence of the 3' fragment precursor for the guanosine transfer reaction. Anti-IGS sequence is highlighted with pink. (c) The sequence of the 5' fragment for the ligation. (d) The sequence of the DNA bridge. (e) Guanosine transfer reaction. (f) Ligation reaction. These reactions were monitored by polyacrylamide gel electrophoresis (PAGE). Reaction components were resolved by PAGE, containing 8 M urea, and stained with SYBR Gold. Arrowheads: (blue) group I intron; (gray) the 3' fragment precursor; (pink) 3' fragment with labeled guanosine; (green) 5' fragment; (black) DNA bridge; (red) labeled RNA (final product) and its reference.

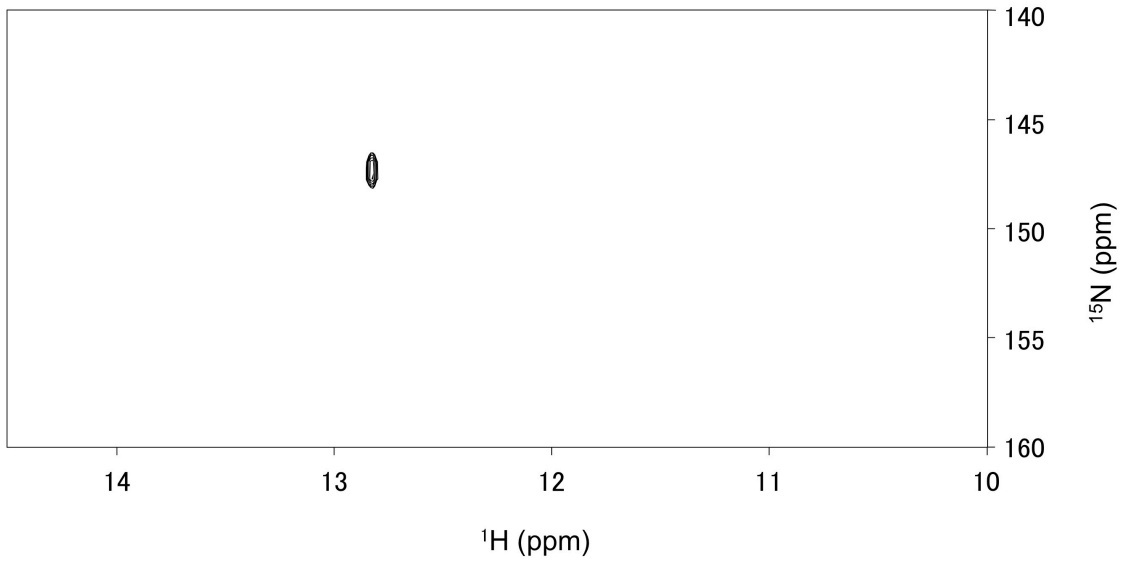

Figure S12. The H1-N1 cross section of the ^{1}H-^{15}N HSQC spectrum of the single-residue labeled 76-nucleotide RNA.

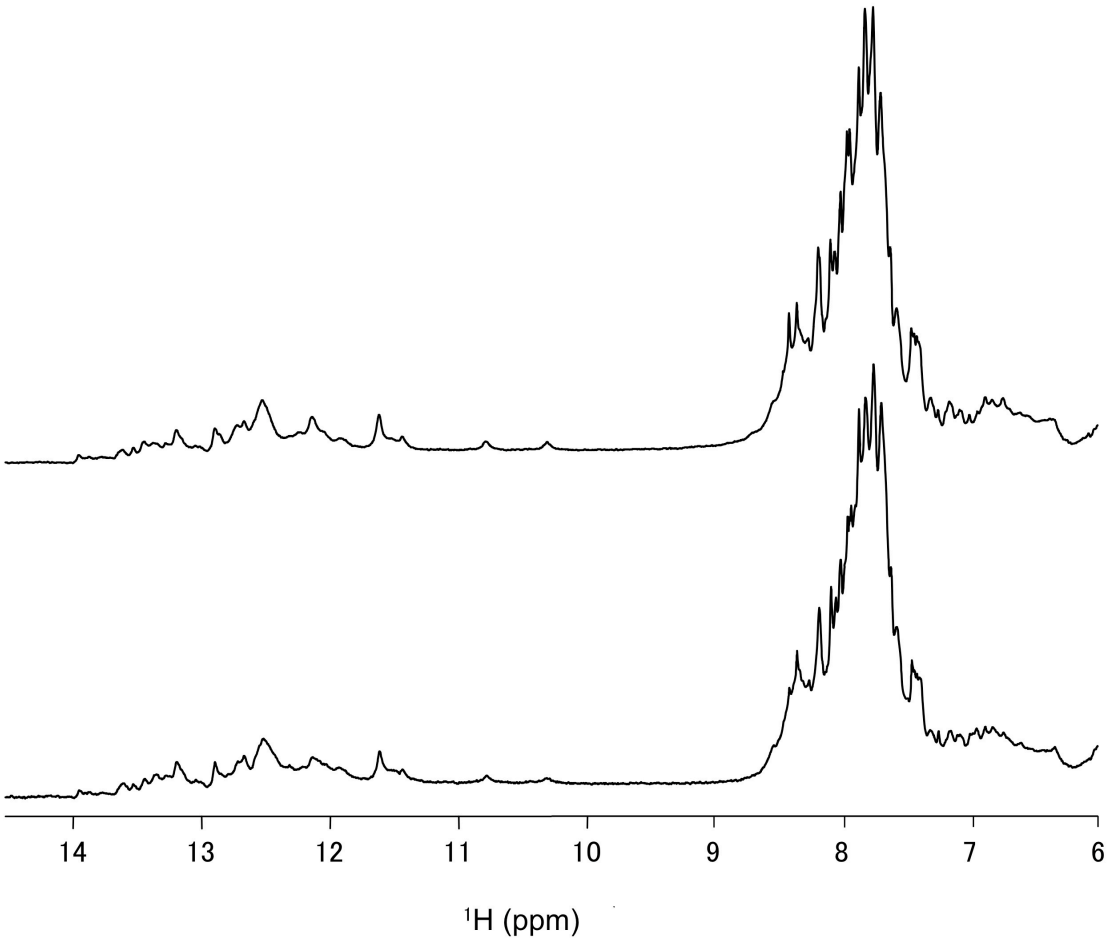

Figure S13. One-dimensional ^{1}H NMR spectra of the non-labeled/single-residue labeled 76-nucleotide RNA. The authentic non-labeled sample (top) and the single-residue labeled sample (bottom). Both spectra were almost identical, which indicates the ^{15}N-labeled and non-labeled samples have the identical sequence.

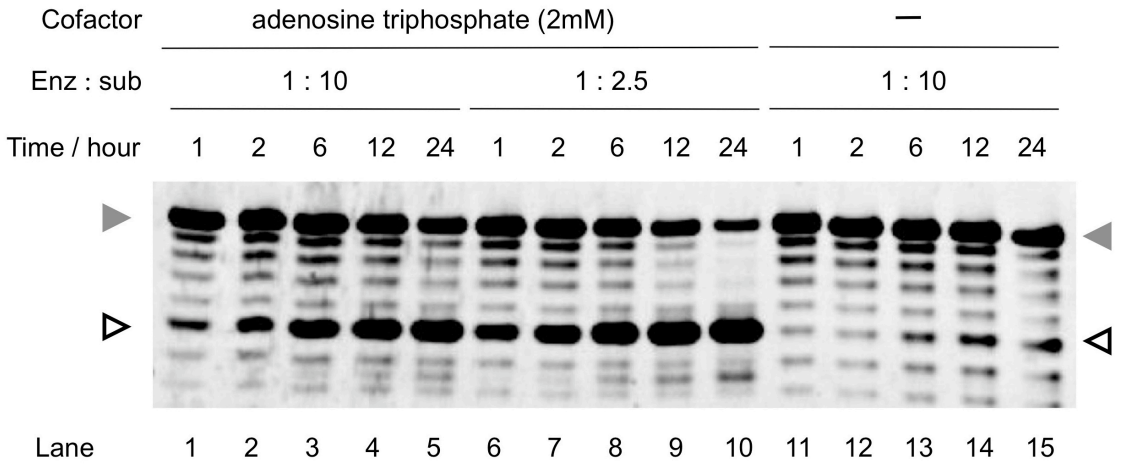

Figure S14. Adenosine transfer reaction. The reaction mixture contained 1.0 μM 3' fragment precursor, 50 mM Tris-HCl pH 7.5, 12 mM $MgCl_2$, and 0.10 or 0.40 μM *Tetrahymena* group I intron in the presence or absence of 2 mM Adenosine 5'-triphosphate (30 μL reaction volume). All reactions were carried out at 37 °C and aliquots taken from reaction mixture were quenched at the indicated time points by adding an equal volume of 75% formamide containing 100 mM EDTA. Gray arrowheads indicate the substrate for the adeniosine transfer reaction and black open arrowheads indicate the processed fragment. The reactions with the adenosine cofactor showed the adenosine transfer reaction efficiently occurred (lanes 1-10), relative to the background hydrolysis (lanes 11-15). The substrate strand for the adenosine transfer was purchased from Japan Bio Service Co., Ltd. (Saitama, Japan). The sequence of the substrate: 5'-(6-FAM)-GGCCCUCUAAAAA. In the adenosine transfer reaction, the substrate strand was processed into the following fragments 5'-FAM-GGCCCUCU and **A**AAAAA where the transferred adenosine reside is shown in bold. Each band was visualized with fluorescent probe (6-FAM) at 5' end of the precursor strand using Pharos FX FluoroImager (BioRad, Hercules, CA).

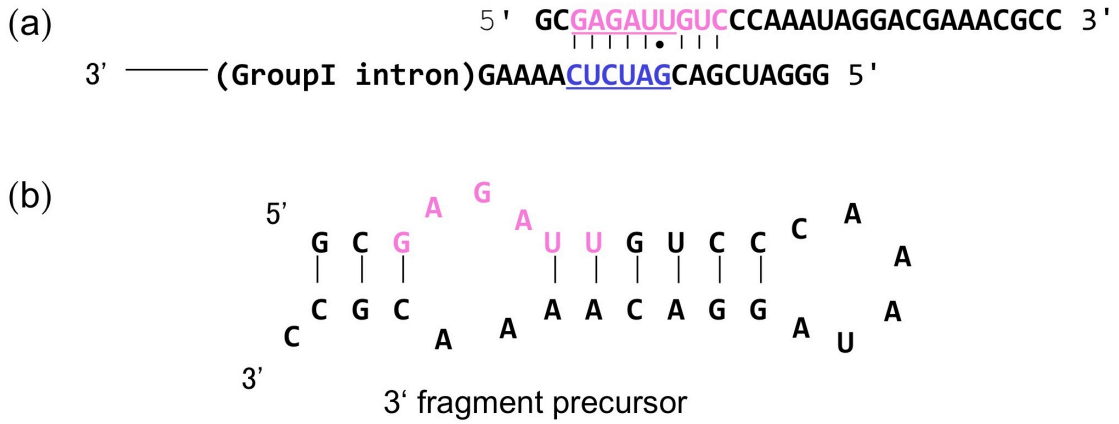

Figure S15. The sequence and the putative secondary structure of the 3'-fragment precursor which inhibited the guanosine transfer reaction. (a) The base-pairing patter between IGS (blue) and anti-IGS (pink) of the 3'-fragment precursor. (b) The putative secondary structure of the 3-fragment precursor.